




Manganese-centered ten-vertex germanium clusters: the strong field Ge₁₀ ligand encapsulating a transition metal

M. M. Uță & R. B. King


To cite this article: M. M. Uță & R. B. King (2015) Manganese-centered ten-vertex germanium clusters: the strong field Ge₁₀ ligand encapsulating a transition metal, Journal of Coordination Chemistry, 68:19, 3485-3497, DOI: [10.1080/00958972.2015.1073267](https://doi.org/10.1080/00958972.2015.1073267)



To link to this article: <http://dx.doi.org/10.1080/00958972.2015.1073267>

 View supplementary material 

 Accepted author version posted online: 21 Jul 2015.
Published online: 18 Aug 2015.

 Submit your article to this journal 

 Article views: 12

 View related articles 

 View Crossmark data 

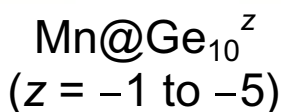
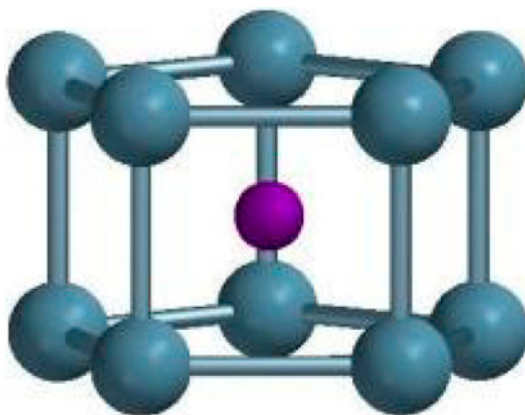
Manganese-centered ten-vertex germanium clusters: the strong field Ge_{10} ligand encapsulating a transition metal

M.M. UȚĂ† and R.B. KING*‡

†Faculty of Chemistry and Chemical Engineering, Babeş-Bolyai University, Cluj–Napoca, Romania

‡Department of Chemistry, University of Georgia, Athens, GA, USA

(Received 26 September 2014; accepted 30 June 2015)



The experimental realization of pentagonal prismatic structures for M@Ge_{10}^{3-} ($\text{M} = \text{Co}, \text{Fe}$) containing interstitial transition metal atoms makes of interest the chemistry of corresponding manganese derivatives Mn@Ge_{10}^z . The neutral Mn@Ge_{10} may be regarded as a complex of a polyhedral Ge_{10}^{2-} ligand with an interstitial Mn in the +2 oxidation state. However, the lowest energy Mn@Ge_{10} structure with the expected sextet spin state for high-spin d^5 Mn(II) lies $\sim 23 \text{ kcal mol}^{-1}$ in energy above the lowest energy isomer thereby suggesting that such germanium polyhedra function as strong field ligands for encapsulated transition metals. The lowest energy structures for the Mn@Ge_{10}^z anions ($z = -1$ to -5) are all centered pentagonal prisms. Higher energy Mn@Ge_{10}^z structures have outer Ge_{10} polyhedra based on the tetracapped trigonal prism similar to the lowest energy Co@Ge_{10}^- structure and on the bicapped square antiprism similar to the $\text{B}_{10}\text{H}_{10}^{2-}$ deltahedron. Other Mn@Ge_{10}^z structures have outer Ge_{10} polyhedra with four or five quadrilateral faces as well as six or eight triangular faces, respectively. Bioctahedral $(\text{Ge}_5)_2\text{Mn}^{5-}$ structures were also found for the pentaanion with a manganese vertex common to two MnGe_5 octahedra. The cationic species Mn@Ge_{10}^+ was found to have a more complicated potential surface than the anions. Tetracapped

*Corresponding author. Email: rbking@chem.uga.edu

trigonal prismatic and bicapped square antiprismatic structures as well as a variety of more open structures were found for Mn@Ge_{10}^+ .

Keywords: Manganese; Germanium; Clusters; Density functional theory; Interstitial atoms

1. Introduction

Bare post-transition metal clusters were first observed by Zintl and co-workers [1–4] in the 1930s during studies of potentiometric titrations of the elements with alkali metals in liquid ammonia. However, such clusters were not characterized structurally until the 1960s when Corbett and co-workers [5] found that complexation of alkali metal counterions with amines or cryptates led to crystalline derivatives of many of the anionic bare post-transition metal clusters suitable for structural characterization by X-ray crystallography.

The original post-transition element clusters were empty clusters containing no interstitial atoms in the centers of the cluster polyhedral. However, subsequent studies led to the discovery of clusters containing interstitial transition metals. Ten-vertex bare post-transition element clusters containing an interstitial atom were found to be of particular interest since such species based on four different 10-vertex polyhedra have been synthesized and characterized structurally by X-ray crystallography (figures 1 and 2). Two of these four polyhedra are deltahedra with all triangular faces (figure 1). These include the D_{4d} bicapped square antiprism encapsulating a metal in the anionic indium cluster Zn@In_{10}^{8-} found in the intermetallic [6] $\text{K}_8\text{In}_{10}\text{Zn}$ as well as in the lead clusters M@Pb_{10}^{2-} found in $[\text{K}(2,2,2\text{-crypt})]_2[\text{M@Pb}_{10}]$ ($\text{M} = \text{Ni}, \text{Pd}, \text{Pt}$) [7, 8]. The other 10-vertex deltahedron is the C_{3v} tetra-capped trigonal prism in the M@In_{10}^{10-} clusters found in the $\text{K}_{10}\text{In}_{10}\text{M}$ intermetallics ($\text{M} = \text{Ni}, \text{Pd}, \text{Pt}$), isoelectronic with Zn@In_{10}^{8-} [9]. The two 10-vertex non-deltahedra encapsulating metal ions (figure 2) include the pentagonal antiprism of bismuth in the cationic bismuth cluster Pd@Bi_{10}^{4+} in $\text{Bi}_{14}\text{PdBr}_{16}$ ($= [\text{Pd@Bi}_{10}][\text{BiBr}_4]_4$) [10] and the pentagonal prism found in the anion Co@Ge_{10}^{3-} of $[\text{K}(2,2,2\text{-crypt})]_4[\text{Co@Ge}_{10}][\text{Co}(1,5\text{-C}_8\text{H}_{12})_2]$ toluene [11] and in the anion Fe@Ge_{10}^{3-} of $[\text{K}(2,2,2\text{-crypt})]_3[\text{Fe@Ge}_{10}]$ [12].

The D_{4d} bicapped square antiprism (figure 1) is the so-called “most spherical” 10-vertex deltahedron [13, 14] found in the deltahedral borane dianion $\text{B}_{10}\text{H}_{10}^{2-}$ having $22 = 2n + 2$ for $n = 10$ skeletal electrons as suggested by the Wade–Mingos rules [15–18] and supported by graph-theory derived models of the skeletal bonding topology [19]. The bicapped square antiprismatic clusters M@Pb_{10}^{2-} ($\text{M} = \text{Ni}, \text{Pd}, \text{Pt}$) and $\text{K}_8\text{In}_{10}\text{Zn}$ are examples of such 22 skeletal electron structures having interstitial atoms in the center of a bicapped square antiprism of post-transition elements. The skeletal electron counting in such systems assumes that the bare post-transition element vertices contribute their valence electrons in excess of a 12-electron filled s^2d^{10} shell. This corresponds to one skeletal electron for an indium vertex and two skeletal electrons for germanium, tin, or lead vertices. The interstitial atom either contributes as skeletal electrons those electrons in excess of the 10-electrons for a filled d^{10} shell or removes the skeletal electrons required to fill a 10-electron d^{10} shell. In the former situation, neutral nickel, palladium, and platinum atoms with exactly filled 10-electron d^{10} shells are donors of zero skeletal electrons whereas interstitial copper and zinc atoms are donors of one and two skeletal electrons, respectively. Using the filled 10-electron d^{10} shell as a criterion for skeletal electron donation makes interstitial cobalt, iron, and manganese atoms acceptors of one, two, and three skeletal electrons, *i.e.* donors of -1 , -2 , and -3 skeletal electrons, respectively.

Until recently the assumption has been made that the preferred polyhedra for metal cluster structures have mainly triangular faces and bear close relationships to the most spherical deltahedra with exclusively triangular faces. Thus the D_{5d} pentagonal antiprism, found experimentally [10] in $\text{Pd}@\text{Bi}_{10}^{4+}$, can be derived from the most spherical 12-vertex deltahedron, namely the regular icosahedron, by removal of an antipodal pair of vertices. This leads to the two parallel pentagonal faces of the pentagonal antiprism in addition to the 10 triangular faces linking the two pentagons. However, the discovery of the clusters $\text{M}@\text{Ge}_{10}^{3-}$ ($\text{M} = \text{Co}$ [11], Fe [12]) with a transition metal ion inside a Ge_{10} pentagonal prism showed that polyhedra with no triangular faces at all can also be the host for encapsulated transition metal ion. Considering an interstitial cobalt to be a one electron acceptor to fill its d^{10} shell makes $\text{Co}@\text{Ge}_{10}^{3-}$ a 22 skeletal electron system expected by the Wade–Mingos rules [15–18] to be a D_{4d} bicapped square antiprism, namely the most spherical 10-vertex deltahedron.

Some clues that D_{5h} pentagonal prismatic structures might be preferred over D_{4d} bicapped square antiprismatic structures for 22 skeletal electron clusters arose from theoretical work occurring contemporaneously with the experimental studies on $\text{M}@\text{Ge}_{10}^{3-}$ ($\text{M} = \text{Co}$ [11], Fe [12]). Thus, density functional theory (DFT) studies on the 22 skeletal electron systems $\text{M}@\text{Ge}_{10}^{2-}$ ($\text{M} = \text{Ni}$, Pd , Pt) predict the pentagonal prismatic structures to be the lowest energy structures for the palladium and platinum derivatives [20]. For the smaller nickel in $\text{Ni}@\text{Ge}_{10}^{2-}$, the D_{4d} structure predicted by the Wade–Mingos rules [15–18] is the lowest energy structure. However, the D_{5h} pentagonal prismatic $\text{Ni}@\text{Ge}_{10}^{2-}$ structure is found to lie only ~ 5 kcal mol $^{-1}$ above the D_{4d} global minimum. The preference for D_{5h} pentagonal prismatic rather than D_{4d} bicapped square prismatic structures for $\text{M}@\text{Ge}_{10}^{2-}$ can be rationalized by the larger internal volume of the pentagonal prism relative to the bicapped square antiprism.

Motivated by the experimentally observed unexpected pentagonal prismatic structures for the $\text{M}@\text{Ge}_{10}^{3-}$ ($\text{M} = \text{Co}$, Fe) trianions, we undertook a comprehensive density theoretical study of $\text{M}@\text{Ge}_{10}^z$ systems with a wide range of charges (z). For the cobalt systems, two particularly favorable structure types emerged from this study [21]. The first was the experimentally observed [11] D_{5h} pentagonal prismatic singlet $\text{Co}@\text{Ge}_{10}^{3-}$ structure, which was found to lie ~ 17 kcal mol $^{-1}$ in energy below the next lowest energy $\text{Co}@\text{Ge}_{10}^{3-}$ structure. Relatively low-energy pentagonal prismatic $\text{Co}@\text{Ge}_{10}^z$ structures with charges (z) ranging from 0 to -5 were also found having doublet to quartet spin states corresponding to adding or subtracting electrons from the singlet $\text{Co}@\text{Ge}_{10}^{3-}$ pentagonal prismatic structure. The second favorable structure type was a C_{3v} singlet tetracapped trigonal prismatic $\text{Co}@\text{Ge}_{10}^-$ structure lying ~ 16 kcal mol $^{-1}$ in energy below the next lowest energy $\text{Co}@\text{Ge}_{10}^-$ structure. This C_{3v} polyhedron is found experimentally in the $\text{M}@\text{In}_{10}^{10-}$ anions in the intermetallics [9] $\text{K}_{10}\text{MIn}_{10}$ ($\text{M} = \text{Ni}$, Pd , Pt), isoelectronic with $\text{Co}@\text{Ge}_{10}^-$. For the iron systems $\text{Fe}@\text{Ge}_{10}^z$, the pentagonal prism was found to be the lowest energy structures in all nine charge states ranging from -5 to $+3$ [22].

A question of interest in interpreting the theoretical results from our studies of $\text{M}@\text{Ge}_{10}^z$ complexes is the nature of the Ge_{10}^z ligand and thus the formal oxidation state of the interstitial transition metal. The spin state of the structure can give a clue regarding the formal transition metal oxidation state. In $\text{Co}@\text{Ge}_{10}^{3-}$, the singlet spin state suggests $\text{Co}(-\text{I})$ with a filled d^{10} shell and thus the outer Ge_{10} pentagonal prism to be a dianionic Ge_{10}^{2-} ligand. A similar interpretation was suggested by Fässler and co-workers in their original experimental paper [11]. Assuming a similar Ge_{10}^{2-} dianionic ligand for the experimentally known [12] pentagonal prismatic $\text{Fe}@\text{Ge}_{10}^{3-}$ suggests the unusual d^9 $\text{Fe}(-1)$ oxidation state for the

central iron. This is consistent with the doublet spin state of the pentagonal prismatic Fe@Ge_{10}^{3-} structure.

Another reason for our theoretical study on Fe@Ge_{10}^z systems was a search for sextet spin state structures having the central iron in the d^5 Fe(III) oxidation state with a favorable half-filled d shell. This would correspond to the Fe@Ge_{10}^+ cation if the outer germanium cluster is assumed to be the Ge_{10}^{2-} dianion similar to the assignment of the Co(-1) formal oxidation state in Co@Ge_{10}^{3-} as discussed above. However, the lowest energy sextet Fe@Ge_{10}^+ structure was found to lie ~ 16 kcal mol $^{-1}$ above the global minimum, which is a doublet structure. This suggests that the Ge_{10}^{2-} cluster surrounding an interstitial transition metal atom functions as a reasonably strong field ligand favoring lower spin states.

The chemistry of manganese is characterized by the very stable high spin d^5 Mn(II) oxidation state with a half-filled d shell and sextet spin multiplicity. Even with the strong field cyanide ion, the tetrahedral Mn(CN)_4^{2-} anion is a high spin sextet [23] suggesting the possibility of low-energy high spin neutral Mn@Ge_{10} structures having the central manganese in the formal Mn(II) oxidation state. Using this rationale, we investigated the complete Mn@Ge_{10}^z series with $z = +1$ to -5 corresponding to manganese formal oxidation states from the d^4 Mn(III) down to the d^{10} Mn(-III). The latter highly negative manganese formal oxidation state is known experimentally in the Mn(CO)_4^{3-} anion [24]. The Mn(-I) formal oxidation state has been encountered in $[\text{Ge}_{10}\text{Mn(CO)}_4]^{3-}$ in which the bicapped square antiprismatic Ge_{10}^{2-} acts as a ligand, in what seems to be the first experimental evidence of the *closo* Ge_{10}^{2-} cluster [25]. An endohedral cluster of D_{2h} symmetry containing a manganese inside a distorted Pb_{12} icosahedron has also been synthesized and reported as $[\text{K}(2,2,2\text{-crypt})]_3[\text{Mn@Pb}_{12}] \cdot 1.5\text{en}$ [26]. Furthermore, recent DFT calculations on M@Ge_{12} systems using various transition metals as central atoms indicate a Ge_{12} icosahedron as the most stable geometry for the Mn@Ge_{12} cluster [27].

The results reported in this paper indicate clearly that Ge_{10}^{2-} functions as a strong field ligand towards an interstitial atom since the lowest energy sextet spin state Mn@Ge_{10} structure is found to lie ~ 23 kcal mol $^{-1}$ in energy above the corresponding global minimum. In addition, the anionic Mn@Ge_{10}^z ($z = -1$ to -5) systems were found to resemble the isoelectronic Fe@Ge_{10}^{z+1} systems since pentagonal prismatic structures were found to be the lowest energy structures in all such systems.

2. Theoretical methods

Geometry optimizations were carried out at the hybrid DFT B3LYP level [28–31] using the 6–31G(d) (valence) double-zeta quality basis functions extended by adding one set of polarization (d) functions for both the interstitial and germanium atoms. For the Mn@Ge_{10}^z ($z = -2$ to $+1$) systems, the four lowest energy identified minima were reoptimized in solvent at the same level of theory. In this connection, CPCM SCRF calculations [32] in tetrahydrofuran (THF) confirm that the gas-phase global minima remain global minima in solution. Adding diffuse functions by the 6-31+G(d) basis set led to convergence problems. Although the resulting minima are similar to some of the ones obtained using the basis set without diffuse functions, a conclusion regarding the energetics in the series of clusters could not be drawn owing to the limited number of structures properly optimized without convergence problems.

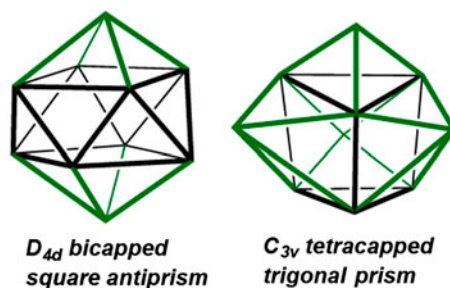


Figure 1. Ten-vertex deltahedra found to encapsulate metal atoms. These deltahedra can be generated by capping rectangular faces of smaller polyhedral. The caps are shown in green and the central polyhedra are shown in black.

The Gaussian 09 package of programs [33] was used in which the fine grid (75,302) is the default for numerically evaluating the integrals and the tight (10^{-8}) Hartree as the default for the self-consistent field convergence. Computations were carried out using six initial geometries, including 10-vertex polyhedra with three-fold, four-fold, and five-fold symmetry encompassing the four polyhedra in figures 1 and 2 as well as a prolate C_{3v} structure and the D_{4h} bicapped cube. The symmetries were maintained during the initial geometry optimization processes. Symmetry breaking using modes defined by imaginary vibrational frequencies was then used to determine optimized structures with minimum energies. Spin states from singlets to sextets were considered. Vibrational analyses show that all of the final optimized structures discussed in this paper are genuine minima at the B3LYP/6-31G(d) level without any significant imaginary frequencies ($N_{\text{imag}} = 0$). In a few cases, the calculations ended with acceptable small imaginary frequencies [34] and these values are indicated in the corresponding figures.

The optimized structures found for the Mn@Ge_{10}^z derivatives are labeled by the numbers of skeletal electrons and their relative energies. In determining the numbers of skeletal electrons, the interstitial manganese is assumed to attain the d^{10} closed-shell configuration by being a three-electron acceptor, *i.e.* a -3 skeletal electron donor. The bare germanium vertices are assumed to be donors of two skeletal electrons each as suggested by the Wade–Mingos rules [15–18]. Spin states are indicated by **S**, **D**, **T**, **Q**, **P**, and **H** for singlet, doublet, triplet, quartet, quintet, and sextet, respectively. Thus, the lowest energy structure of the singlet pentaanion Mn@Ge_{10}^{5-} is labeled **22–1S**.

Additional details of all of the optimized structures listing all interatomic distances, the initial geometries leading to a given optimized structure, and structures with energies too

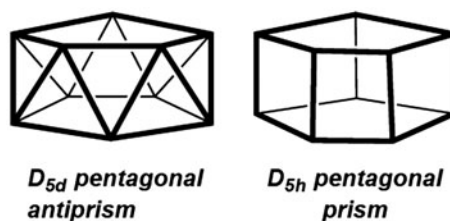


Figure 2. Ten-vertex non-deltahedra found to encapsulate metal atoms.

high to be of possible chemical relevance are provided in the Supporting Information. In assigning polyhedra to the optimized structures, the Ge–Ge distances less than ~ 3.3 Å were normally considered as polyhedral edges; significant exceptions are noted in the text. Similarly Mn–Ge distances less than ~ 2.8 Å were considered bonding distances; most such Mn–Ge bonding distances were less than ~ 2.5 Å except for some of the less regular polyhedral structures.

3. Results and discussion

3.1. Neutral Mn@Ge₁₀

The manganese atom in neutral Mn@Ge₁₀ is in the d⁵ formal Mn(II) oxidation state if the Ge₁₀²⁻ cluster is assumed to be the dianion as discussed above. The lowest energy high spin sextet Mn@Ge₁₀ cluster **17-4H** has a *D*_{4d} bicapped square antiprism structure for the outer Ge₁₀ unit (figures 1 and 3). The Wade–Mingos rules [15–18] suggest $2n + 2$ skeletal electrons for such a structure consistent with a Ge₁₀²⁻ dianion and thus a d⁵ Mn(II) formal oxidation state. However, this high spin structure **17-4H** lies 23.1 kcal mol⁻¹ above the lowest energy Mn@Ge₁₀ structure **17-1Q**. The optimization in THF leads to a similar result, with an energy difference of 22.9 kcal mol⁻¹ between the *D*_{4d} bicapped square antiprism structure and the *C*_{3v} global minimum. This suggests that the Ge₁₀²⁻ ligand functions as a strong field ligand to an interstitial manganese atom.

The lowest energy Mn@Ge₁₀ structure **17-1Q** is a quartet *C*_{3v} structure based on a tetracapped trigonal prism (figure 3). A slightly higher energy doublet Mn@Ge₁₀ structure **17-2D**, lying 1.9 kcal mol⁻¹ above **17-1Q**, is also found based on similar tetracapped trigonal prism topology. However, in **17-2D** the ideal *C*_{3v} symmetry of the tetracapped trigonal prism is distorted to *C*_s symmetry. Both of these structures were also found in the optimizations in THF, with a lower energy gap of 1.5 kcal mol⁻¹ between them. The remaining low-energy Mn@Ge₁₀ structure is the pentagonal prismatic structure **17-3D**, lying 4.3 kcal mol⁻¹ above **17-1Q**. In **17-3D**, the ideal *D*_{5h} symmetry of the Ge₁₀ pentagonal prism is distorted to *C*_s symmetry. In this distorted structure, the edge lengths of the pentagonal faces range from 2.44 to 2.63 Å.

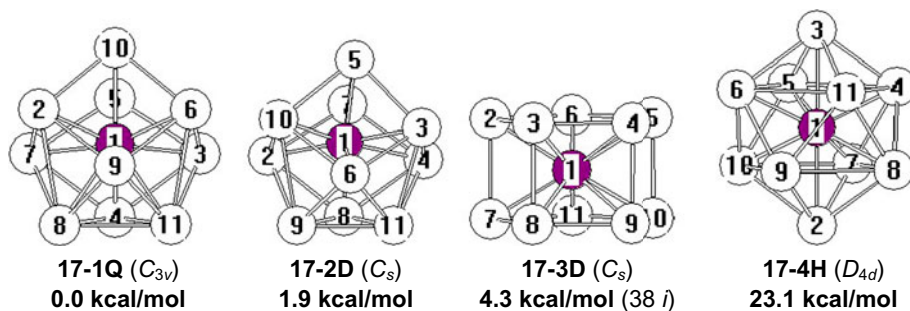


Figure 3. The four optimized Mn@Ge₁₀ structures within 25 kcal mol⁻¹ of the global minimum.

3.2. Anionic Mn@Ge_{10}^z derivatives ($z = -1$ to -5)

The lowest energy structures for the Mn@Ge_{10}^z anions ($z = -1$ to -5) are all pentagonal prisms with triplet ($z = -1$), quartet ($z = -2$), triplet ($z = -3$), doublet ($z = -4$), and singlet ($z = -5$) spin states (figures 4–7). Ideal D_{5h} symmetry is retained for the Ge_{10} polyhedra in all of these structures except for the dianion Mn@Ge_{10}^{2-} (**19–1Q** in figure 5) in which the edge lengths of the pentagonal faces range from 2.44 to 2.63 Å. Structure **20–1T** has an outer regular Ge_{10} pentagonal prism but with the manganese not located at the center of the polyhedron as indicated by Mn–Ge distances ranging from 2.464 to 2.606 Å. The singlet pentaanion Mn@Ge_{10}^{5-} (**22–1S** in figure 7) is a closed shell structure and is isoelectronic with the experimentally known [11] Co@Ge_{10}^{3-} . The doublet Mn@Ge_{10}^{4-} structure **21–1D** (similar to **22–1S** in figure 7 and therefore not depicted in a separate figure) is isoelectronic with the known [12] Fe@Ge_{10}^{3-} . Structure **21–1D** appears to be unusually favorable since it lies a very large ~ 42 kcal mol $^{-1}$ in energy below the next lowest energy Mn@Ge_{10}^{4-} structure. For Mn@Ge_{10}^{3-} , a singlet pentagonal prismatic structure **20–2S** with ideal D_{5h} symmetry similar to the isomeric triplet structure **20–1S** lies 14.5 kcal mol $^{-1}$ above **20–1S**. Similarly, for Mn@Ge_{10}^{-} , a singlet pentagonal prismatic structure **18–2S** lies 2.5 kcal mol $^{-1}$ in energy above **18–1T** (figure 4). However, **18–2S** is distorted from ideal D_{5h} symmetry to C_{2v} symmetry with pentagonal face edge lengths ranging from 2.44 to 2.65 Å. Optimizations in THF lead to the same three structures in order of energy for the Mn@Ge_{10}^{-} clusters, starting with the D_{5h} symmetry global minimum, in the same energy range. The difference in relative energies between the two equivalent series is about 0.1 kcal mol $^{-1}$.

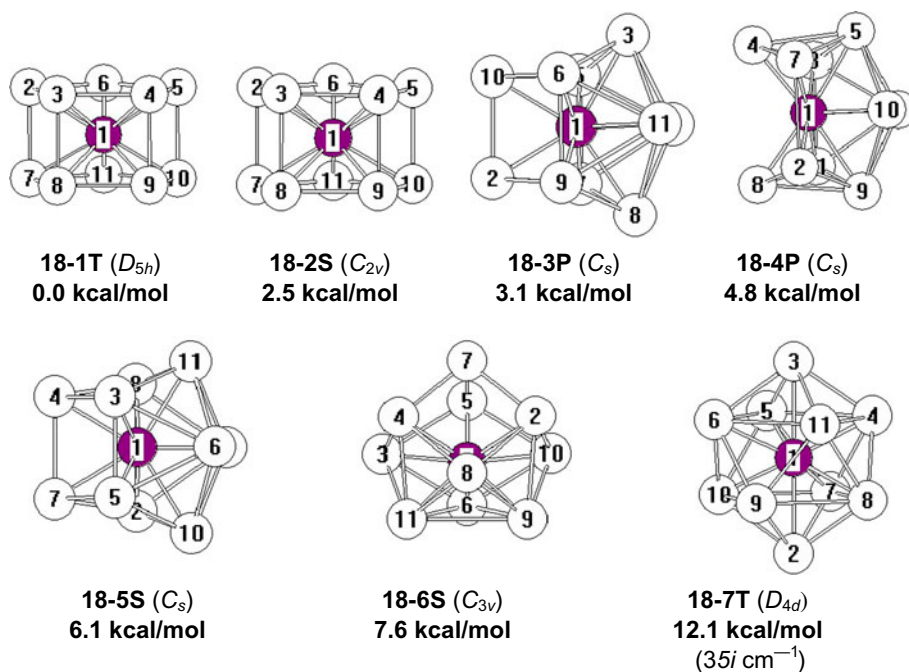


Figure 4. The seven optimized Mn@Ge_{10} structures within 25 kcal mol $^{-1}$ of the global minimum.

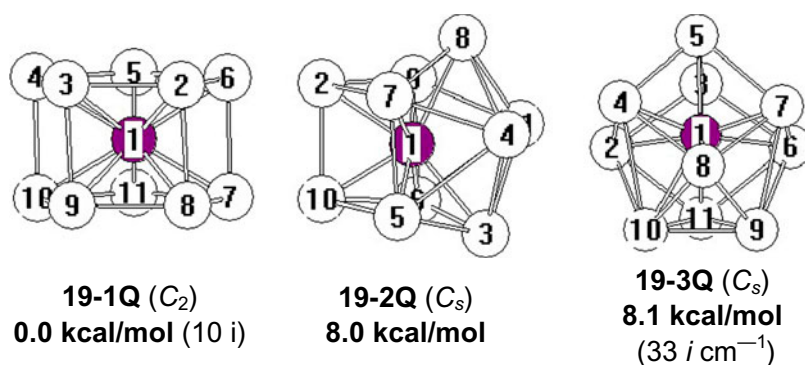


Figure 5. The three optimized $Mn@Ge_{10}^{2-}$ structures within 25 kcal mol $^{-1}$ of the global minimum.

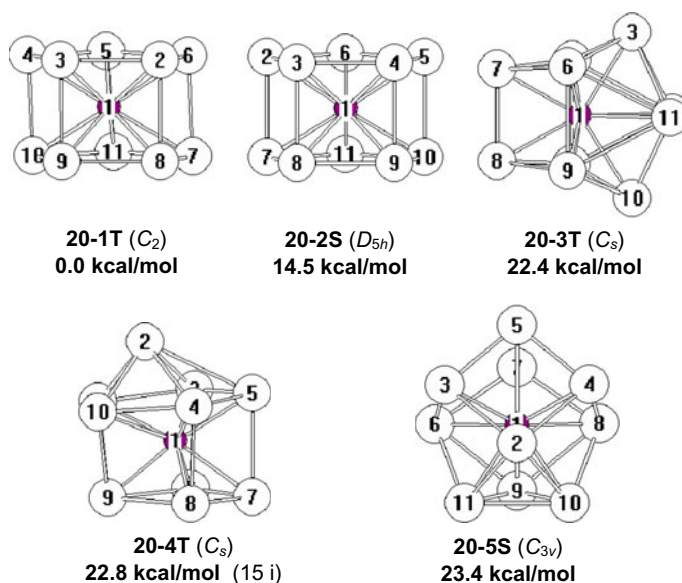


Figure 6. The five optimized $Mn@Ge_{10}^{3-}$ structures within 25 kcal mol $^{-1}$ of the global minimum.

The occurrence of pentagonal prisms rather than polyhedra with triangular faces in $M@Ge_{10}^z$ structures relates to the large volume of the pentagonal prism relative to other 10-vertex polyhedra for encapsulating a central metal. Thus, removal of edges to convert pairs of triangular faces to quadrilateral faces or trios of triangular faces to pentagonal faces increases the volume of the Ge_{10} polyhedron to accommodate an interstitial atom. A less extreme removal of edges to increase the volume of a Ge_{10} polyhedron is found in the $Mn@Ge_{10}^-$ structures **18-3P** and **18-5S** (figure 4), the $Mn@Ge_{10}^{2-}$ structure **19-2Q** (figure 5), the $Mn@Ge_{10}^{3-}$ structure **20-3T** (figure 6), and the $Mn@Ge_{10}^{5-}$ structure **22-7T** (figure 7) lying 3.1, 4.8, 8.0, 22.4, and 22.6 kcal mol $^{-1}$, respectively, above the corresponding isomeric lowest energy structures. The Ge_{10} polyhedra in these structures have two rectangular faces,

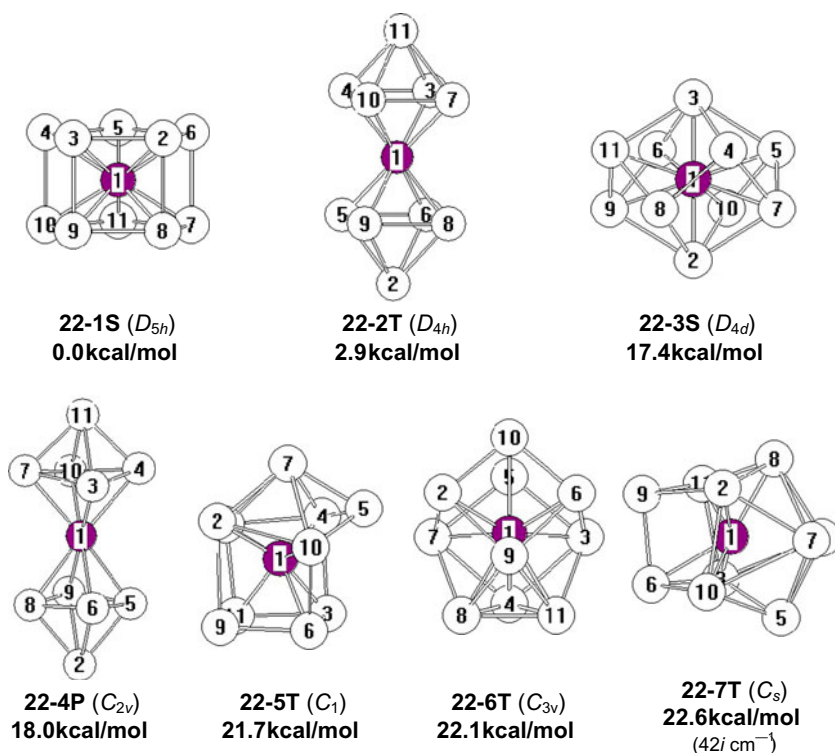


Figure 7. The seven optimized $Mn@Ge_{10}^{5-}$ structures within 25 kcal mol⁻¹ of the global minimum.

two concave quadrilateral faces, and eight triangular faces and thus are conveniently designated as “4f₄ polyhedra”. This corresponds to two degree three vertices, six degree four vertices, and two degree five vertices. The Ge₁₀ polyhedron in the quintet $Mn@Ge_{10}^-$ **18-4P** is also related to the 4f₄ polyhedron by lengthening one of the edges. Another slightly more open polyhedron, found in the triplet $Mn@Ge_{10}^{3-}$ structure **20-4T** lying 22.8 kcal mol⁻¹ above **20-1T**, has four approximately rectangular faces, one quadrilateral face, and six triangular faces, and thus is conveniently designated as a “5f₄ polyhedron” (figure 6). The energies of the 4f₄ polyhedral $Mn@Ge_{10}^{z-}$ structures relative to the isomeric pentagonal prismatic structures increase as z becomes more negative. This may relate to the effectively larger size of the interstitial manganese as the negative charge is increased thereby requiring a larger cavity inside the outer Ge₁₀ polyhedron.

A singlet C_{3v} structure based on the tetrapped trigonal prism was found to be the lowest energy structure for the $Co@Ge_{10}^-$ monoanion as well as neutral $Co@Ge_{10}$ [21]. In the isoelectronic $Mn@Ge_{10}^{3-}$ trianion an analogous C_{3v} structure **20-5S** is found, but at the relatively high energy of 23.4 kcal mol⁻¹ above the lowest energy isomer **20-1T**. Other tetrapped trigonal prism structures of $Mn@Ge_{10}^{z-}$ systems include the singlet $Mn@Ge_{10}^-$ structure **18-6S**, the quartet $Mn@Ge_{10}^{2-}$ structure **19-3Q**, and the triplet $Mn@Ge_{10}^{5-}$ structure **22-6T**, lying 7.6, 8.1, and 22.1 kcal mol⁻¹ in energy, respectively, above the corresponding minimum energy isomers. Ideal C_{3v} symmetry is maintained for the tetrapped trigonal prisms in **18-6S**, **20-5S**, and **22-6T**. However, for the quartet $Mn@Ge_{10}^{2-}$ dianion structure

19–3Q the ideal C_{3v} structure is distorted to C_s symmetry with edge-length deviations from ideal symmetry up to ~ 0.06 Å. A similar deviation from ideal C_{3v} symmetry is not found in the isoelectronic Co@Ge_{10} structure, which, however, is a low-spin doublet rather than the tetracapped trigonal prism quartet spin state **19–3Q** [21]. No tetracapped trigonal prism structure was found for the tetraanion Mn@Ge_{10}^{4-} at accessible energies.

The interpretation of the Mn@Ge_{10}^{z-} structures as manganese complexes of a surrounding Ge_{10} ligand considers the ligand as the Ge_{10}^{2-} dianion. The preferred structure for an empty Ge_{10}^{2-} dianion is the D_{4d} bicapped square antiprism similar to the well-known $\text{B}_{10}\text{H}_{10}^{2-}$ deltahedron. In all of the lowest energy Mn@Ge_{10}^{z-} structures, this deltahedron opens up to a polyhedron with a larger internal volume and non-triangular faces to accommodate the interstitial manganese. The extreme example of such deltahedral opening retaining a true polyhedral structure is the pentagonal prism as discussed above. However, some higher energy Mn@Ge_{10}^{z-} structures are found retaining the bicapped square antiprism geometry and D_{4d} symmetry of the Ge_{10} polyhedron. These include the triplet Mn@Ge_{10}^{-} structure **18–7T** (figure 4) and the singlet Mn@Ge_{10}^{5-} structure **22–3S** (figure 7) lying 12.1 and 17.4 kcal mol $^{-1}$, respectively, above the lowest energy isomers. In the monoanion **18–7T**, the eight edges of the square faces of the underlying square antiprism are relatively long at 3.107 Å with the edges connecting the two square faces at 2.700 Å. In the pentaanion **22–3S**, the eight edges of the square faces of the underlying square antiprism are expanded to non-bonding distances of 3.490 Å to obtain a large volume of the interstitial atom. This expansion leads to compression of the distances of the edges connecting the two square faces to 2.483 Å.

Alternatives to Mn@Ge_{10}^{z-} structures consisting of an outer Ge_{10} polyhedron surrounding an interstitial manganese are isomeric structures having two polyhedra sharing a manganese vertex. Examples of such structures are the triplet $(\text{Ge}_5)_2\text{Mn}^{5-}$ structure **22–2T** and the quintet structure **22–4P**, lying 2.9 and 18.0 kcal mol $^{-1}$ above the lowest energy Mn@Ge_{10}^{5-} isomer **22–1S** (figure 7). In these structures two MnGe_5 suboctahedra share the manganese vertex. The triplet structure **22–2T** has ideal D_{4h} symmetry, retaining the C_4 axis common to both MnGe_5 suboctahedra in this structure. However, in the quintet structure **22–4P** the C_4 axes of each MnGe_5 suboctahedron are preserved but one of the suboctahedra is larger than the other suboctahedron. A very high energy singlet spin state $(\text{Ge}_5)_2\text{Mn}^{5-}$ structure is also found with the ideal D_{4h} symmetry lying at the very high energy of 37.8 kcal mol $^{-1}$ relative to **22–1S**.

3.3. The Mn@Ge_{10}^+ cation

The potential energy surfaces of the Mn@Ge_{10}^{z+} cations are significantly more complicated than those of the Mn@Ge_{10}^{z-} anion with a larger number of low-energy structures. The Ge_{10} polyhedra in many of the low-energy structures of the Mn@Ge_{10}^{z+} cations are low-symmetry not readily recognizable open polyhedra. As an example, the four lowest energy structures of the Mn@Ge_{10}^+ monocation are shown in figure 8. The lowest energy Mn@Ge_{10}^+ structure **16–1S** is a singlet spin state distorted tetracapped trigonal prism, which can be obtained by removal of an electron from the doublet Mn@Ge_{10} structure **17–1D**. The next Mn@Ge_{10}^+ structure **16–2P**, lying 2.4 kcal mol $^{-1}$ in energy above **16–1S**, is a quintet spin state bicapped square antiprism retaining the ideal D_{4d} symmetry. Computations in THF reveal this structure at a slightly higher relative energy of 3.7 kcal mol $^{-1}$ above the same singlet distorted tetracapped trigonal prism global minimum. In **16–2P**, the edge lengths of the two square faces of the underlying square antiprism are 3.220 Å whereas the lengths of the edges connecting these two square faces are 2.734 Å. The Mn@Ge_{10}^+ structure **16–4P**, lying 4.4 kcal mol $^{-1}$ in energy

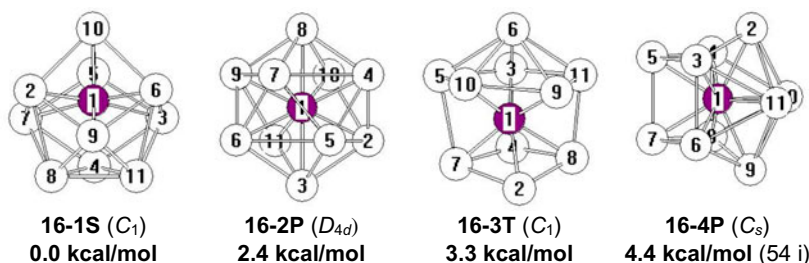


Figure 8. The four optimized $Mn@Ge_{10}^+$ structures within 8 kcal mol^{-1} of the global minimum.

above **16-1S**, is a quintet spin state structure with an outer $4f_4$ Ge_{10} polyhedron similar to the $4f_4$ polyhedra in the anionic structures **18-3P**, **18-5S**, **19-2Q**, **20-3T**, and **22-7T** discussed above. The final low-energy $Mn@Ge_{10}^+$ structure, namely the triplet spin state **16-3T** lying $3.3 \text{ kcal mol}^{-1}$ in energy above **16-1S**, has an open outer Ge_{10} polyhedron with an open non-planar heptagonal face (Ge atoms 2-7-5-10-9-11-8 in figure 8).

4. Summary

The neutral species $Mn@Ge_{10}$ can be interpreted as a Mn(II) complex of a Ge_{10}^{2-} ligand completely surrounding the interstitial manganese. However, the lowest energy $Mn@Ge_{10}$ structure corresponding to the sextet spin state of high spin d^5 Mn(II) lies $\sim 23 \text{ kcal mol}^{-1}$ in energy above the lowest energy isomer, which is a quartet C_{3v} structure based on a tetracapped trigonal prism. The Ge_{10} “ligand” polyhedron in the sextet $Mn@Ge_{10}$ structure is an undistorted D_{4d} bicapped square antiprism similar to the $B_{10}H_{10}^{2-}$ deltahedron. This is consistent with its formulation as a dianionic ligand complexing with the interstitial Mn(II). These observations indicate quite clearly that a Ge_{10}^{2-} ligand surrounding completely an interstitial transition metal atom functions as a strong field ligand.

Investigation of the anionic species $Mn@Ge_{10}^z$ ($z = -1$ to -5) shows pentagonal prismatic structures similar to the experimental $M@Ge_{10}^{3-}$ structures ($M = Co$ [11], Fe [12]) to be the lowest energy structures in all cases. Higher energy $Mn@Ge_{10}^z$ structures include structures with outer Ge_{10} polyhedra based on the tetracapped trigonal prism similar to the lowest energy $Co@Ge_{10}^-$ structure and on the bicapped square antiprism similar to the $B_{10}H_{10}^{2-}$ deltahedron. Other $Mn@Ge_{10}^z$ structures have outer Ge_{10} polyhedra with four or five quadrilateral faces as well as six or eight triangular faces, respectively. Biocuboctahedral $(Ge_5)_2Mn^{5-}$ structures were also found for the pentaanion with the manganese vertex common to two $MnGe_5$ octahedra. The cationic species $Mn@Ge_{10}^+$ was found to have a more complicated potential surface than the anionic species. Tetracapped trigonal prismatic and bicapped square antiprismatic structures as well as a variety of more open structures were found for $Mn@Ge_{10}^+$.

Supporting information available

Tables of distances for the $Mn@Ge_{10}^z$ derivatives ($z = -5$ to $+1$); tables of distances for the $Mn@Ge_{10}^z$ derivatives in THF ($z = -2$ to $+1$); tables of distances for the few $Mn@Ge_{10}^z$

derivatives optimized using the B3LYP/6-31+G(d) basis set ($z = -2$ to $+1$); complete Gaussian reference (reference [33]).

Disclosure statement

No potential conflict of interest was reported by the authors.

Funding

This work was supported by Babeş-Bolyai University from the program of grants for young researchers [grant number GTC 34043/2013].

Supplemental data

Supplemental data for this article can be accessed here [<http://dx.doi.org/10.1080/00958972.2015.1073267>].

References

- [1] E. Zintl, J. Goubeau, W. Dullenkopf. *Z. Phys. Chem. Abt. A*, **154**, 1 (1931).
- [2] E. Zintl, A. Harder. *Z. Phys. Chem. Abt. A*, **154**, 47 (1931).
- [3] E. Zintl, W. Dullenkopf. *Z. Phys. Chem. Abt. B*, **16**, 183 (1932).
- [4] E. Zintl, H. Kaiser. *Z. Anorg. Allg. Chem.*, **211**, 113 (1933).
- [5] J.D. Corbett. *Chem. Rev.*, **85**, 383 (1985).
- [6] S.C. Sevov, J.C. Corbett. *Inorg. Chem.*, **32**, 1059 (1993).
- [7] E.N. Esenturk, J. Fettingner, B. Eichhorn. *Chem. Commun.*, **2**, 247 (2005).
- [8] E.N. Esenturk, J. Fettingner, B. Eichhorn. *J. Am. Chem. Soc.*, **128**, 9178 (2006).
- [9] R.W. Henning, J.D. Corbett. *Inorg. Chem.*, **38**, 3883 (1999).
- [10] M. Ruck, V. Dubenskyy, T. Söhnel. *Angew. Chem. Int. Ed.*, **42**, 2978 (2003).
- [11] J.-Q. Wang, S. Stegmaier, T.F. Fässler. *Angew. Chem. Int. Ed.*, **48**, 1998 (2009).
- [12] B. Zhou, M.S. Denning, D.L. Kays, J.M. Goicoechea. *J. Am. Chem. Soc.*, **131**, 2802 (2009).
- [13] R.E. Williams. *Inorg. Chem.*, **10**, 210 (1971).
- [14] R.E. Williams. *Chem. Rev.*, **92**, 177 (1992).
- [15] K. Wade. *Chem. Commun.*, **15**, 792 (1971).
- [16] K. Wade. *Adv. Inorg. Chem. Radiochem.*, **18**, 1 (1976).
- [17] D.M.P. Mingos. *Nature Phys. Sci.*, **99**, 236 (1972).
- [18] D.M.P. Mingos. *Acc. Chem. Res.*, **17**, 311 (1984).
- [19] R.B. King, D.H. Rouvray. *J. Am. Chem. Soc.*, **99**, 7834 (1977).
- [20] R.B. King, I. Silaghi-Dumitrescu, M.M. Uță. *J. Phys. Chem. A*, **113**, 527 (2009).
- [21] M.M. Uță, D. Cioloboc, R.B. King. *Inorg. Chem.*, **51**, 3498 (2012).
- [22] M. Uță, D. Cioloboc, R.B. King. *J. Phys. Chem. A*, **116**, 9197 (2012).
- [23] W.E. Buschmann, A.M. Arif, J.S. Miller. *Angew. Chem. Int. Ed.*, **37**, 781 (1998).
- [24] J.E. Ellis, R.A. Faltynek. *J. Am. Chem. Soc.*, **99**, 1801 (1977).
- [25] D. Rios, S.C. Sevov. *Inorg. Chem.*, **49**, 6396 (2010).
- [26] B. Zhou, T. Krämer, A.L. Thompson, J.E. McGrady, J.M. Goicoechea. *Inorg. Chem.*, **50**, 8028 (2011).
- [27] J.M. Goicoechea, J.E. McGrady. *Dalton Trans.*, **44**, 6755 (2015).
- [28] S.H. Vosko, L. Wilk, M. Nusair. *Can. J. Phys.*, **58**, 1200 (1980).
- [29] C. Lee, W. Yang, R.G. Parr. *Phys. Rev. B*, **37**, 785 (1988).
- [30] A.D. Becke. *J. Chem. Phys.*, **98**, 5648 (1993).
- [31] P.J. Stephens, F.J. Devlin, C.F. Chabalowski, M.J. Frisch. *J. Phys. Chem.*, **98**, 11623 (1994).
- [32] A. Klamt, G. Schüürmann. *J. Chem. Soc., Perkin Trans. 2*, **5**, 799 (1993).
- [33] M.J. Frisch, G.W. Trucks, H.B. Schlegel, G.E. Scuseria, M.A. Robb, J.R. Cheeseman, G. Scalmani, V. Barone, B. Mennucci, G.A. Petersson, H. Nakatsuji, M. Caricato, X. Li, H.P. Hratchian, A.F. Izmaylov, J. Bloino, G. Zheng, J.L. Sonnenberg, M. Hada, M. Ehara, K. Toyota, R. Fukuda, J. Hasegawa, M. Ishida, T. Nakajima, Y. Honda, O. Kitao, H. Nakai, T. Vreven, J.A. Montgomery Jr., J.E. Peralta, F. Ogliaro, M. Bearpark, J.J. Heyd,

- E. Brothers, K.N. Kudin, V.N. Staroverov, R. Kobayashi, J. Normand, K. Raghavachari, A. Rendell, J.C. Burant, S.S. Iyengar, J. Tomasi, M. Cossi, N. Rega, J.M. Millam, M. Klene, J.E. Knox, J.B. Cross, V. Bakken, C. Adamo, J. Jaramillo, R. Gomperts, R.E. Stratmann, O. Yazyev, A.J. Austin, R. Cammi, C. Pomelli, J.W. Ochterski, R.L. Martin, K. Morokuma, V.G. Zakrzewski, G.A. Voth, P. Salvador, J.J. Dannenberg, S. Dapprich, A.D. Daniels, O. Farkas, J.B. Foresman, J.V. Ortiz, J. Cioslowski, D.J. Fox, *Gaussian 09, Revision A.02*, Gaussian, Wallingford, CT (2009). (see Supporting Information for details).
- [34] Y. Xie, H.F. Schaefer, R.B. King. *J. Am. Chem. Soc.*, **122**, 8746 (2000).